BBA - Bioenergetics 1864 (2023) 148977

Contents lists available at ScienceDirect

BBA - Bioenergetics

journal homepage: www.elsevier.com/locate/bbabio

Two separate pathways underlie NADH and succinate oxidation in swine heart mitochondria: Kinetic evidence on the mobile electron carriers

Salvatore Nesci [a,*,1], Cristina Algieri [a,1], Fabiana Trombetti [a], Micaela Fabbri [a], Giorgio Lenaz [b]

[a] Department of Veterinary Medical Sciences, University of Bologna, Via Tolara di Sopra 50, 40064 Ozzano Emilia, BO, Italy
[b] Department of Biomedical and Neuromotor Sciences, University of Bologna, Via Massarenti 9, Pad 11, 40138 Bologna, BO, Italy

ARTICLE INFO

Keywords:
Mitochondria
Supercomplexes
Channelling
Coenzyme Q
Cytochrome *c*
Metabolic flux control

ABSTRACT

We have investigated NADH and succinate aerobic oxidation in frozen and thawed swine heart mitochondria. Simultaneous oxidation of NADH and succinate showed complete additivity under a variety of experimental conditions, suggesting that the electron fluxes originating from NADH and succinate are completely independent and do not mix at the level of the so-called mobile diffusible components. We ascribe the results to mixing of the fluxes at the level of cytochrome *c* in bovine mitochondria: the Complex IV flux control coefficient in NADH oxidation was high in swine mitochondria but very low in bovine mitochondria, suggesting a stronger interaction of cytochrome *c* with the supercomplex in the former. This was not the case in succinate oxidation, in which Complex IV exerted little control also in swine mitochondria. We interpret the data in swine mitochondria as restriction of the NADH flux by channelling within the I-III_2-IV supercomplex, whereas the flux from succinate shows pool mixing for both Coenzyme Q and probably cytochrome *c*. The difference between the two types of mitochondria may be ascribed to different lipid composition affecting the cytochrome *c* binding properties, as suggested by breaks in Arrhenius plots of Complex IV activity occurring at higher temperatures in bovine mitochondria.

1. Introduction

The notion of mobile diffusible redox carriers (Coenzyme Q (CoQ) and cytochrome *c* (cyt *c*)) in the inner mitochondrial membrane as the vehicle of electrons from respiratory complexes [1] has somewhat changed with the discovery of respiratory supramolecular units, in particular, the supercomplexes (SCs) comprising Complexes I (CI), III (CIII) and IV (CIV) [2]; in such assemblies, the electron transfer was proposed [2] to be mediated by channelling of CoQ between CI and CIII, and of cyt *c* between CIII and CIV, with a clear kinetic advantage on the transfer based on random collisions. The proximity of the CoQ-reducing site in CI with the $CoQH_2$-oxidizing site in CIII in the SC (*e.g.* [3]) added further favour to this suggestion. Furthermore, evidence for channelling between CI and CIII has been produced in our laboratory exploiting metabolic control analysis in bovine heart submitochondrial particles [4] and *in vitro* reconstitution studies [5], whereas electron transfer between Complex II (CII) and CIII followed a random collision behaviour. Our studies showed that CI and CIII kinetically behave as a single unit and that SC formation provides a rate advantage over collision-based diffusion-mediated electron transfer in the CoQ region [6]. Contrary to the CoQ region, the flux control studies of Bianchi et al. [4] showed low flux control of CIV, suggesting that electron transfer follows pool behaviour in the cyt *c* region. Since in bovine heart mitochondria CIV is present in large amounts in free form besides in SCs, we have interpreted these results with possible masking of channelled flux between CIII and CIV by a large amount of free CIV [7]. Nevertheless, channelling of cyt *c* between CIII and CIV has been suggested by a number of investigations, reviewed by Nesci and Lenaz [8].

On the other hand studies by Enriquez and coworkers by the isolation of SCs in active form [9] and by genetic manipulation modulating the contents of the respiratory chain components [10] strongly suggest the existence of two separate pools of CoQ, one dedicated to NADH oxidation within the ($CICIII_2$) SC and the other one dedicated to oxidation of succinate (and other FAD-linked substrates, such as Electron Transfer

Abbreviations: CoQ, Coenzyme Q; cyt *c*, cytochrome *c*; SCs, supercomplexes; CI, Complexes I; CII, Complexes II; CIII, Complexes III; CIV, Complexes IV; AA, Antimycin A; ASC, ascorbate; TMPD, *N*,*N*,*N*′,*N*′-tetramethyl-*p*-phenylenediamine dihydrochloride; DDM, n-dodecyl-β-D-maltoside.

* Corresponding author at: via Tolara di Sopra – 50, 40064 Ozzano Emilia, BO, Italy.
E-mail address: salvatore.nesci@unibo.it (S. Nesci).

[1] These authors contributed equally.

https://doi.org/10.1016/j.bbabio.2023.148977
Received 14 November 2022; Received in revised form 25 March 2023; Accepted 6 April 2023
Available online 12 April 2023

Flavoprotein), that is freely mobile in the phospholipid bilayer of the inner mitochondrial membrane [11]. If this is the case, then adding either NADH or succinate to mitochondrial membranes should reduce only part of the CIII population, whereas adding both simultaneously should reduce the whole population. If the CoQ pool is not partitioned into two (a single pool is accessible to all enzymes), then adding NADH or succinate alone should reduce the whole population directly. In the former case, the NADH and succinate activities would be additive, whereas, in the latter case, the combined activity would be less than the individual rates.

Blaza et al. [12] have systematically criticized all previous evidence in favour of channelling on the basis of the following experimental argumentations: (*i*) they found that steady-state aerobic NADH and succinate oxidation, as well as reduction of cyt *c* by these two substrates in bovine heart submitochondrial particles, show incomplete additivity in their experimental conditions, in contrast with what expected by the existence of separate pathways involving two subsets of CoQ and in accordance with the idea of a single homogeneous pool of the quinone that was suggested by the older kinetic analysis of Kröger and Klingenberg [13] and in accordance with the "Random Collision Model" [14]; (*ii*) Blaza et al. [12] refute the metabolic flux control analysis of Bianchi et al. [4] on the basis that rotenone is competitive with CoQ and therefore the extent of its inhibition of CI may be affected by the additional presence of the exogenous quinone employed in CI assay but absent in the assay of NADH aerobic oxidation. In other words, the simultaneous presence of NADH and succinate add more than the individual addition of substrates. This observation is not in agreement with the full existence of separate pathways. Therefore, the high flux control coefficient of CI found by Bianchi et al. [4] by using rotenone inhibition was rejected as an artefact. As a conclusion, Blaza et al. [12] propose that SCs, though present as real entities, do not have any functional role in electron transfer.

Hirst's group [15] has subsequently provided additional criticism to the concept of CoQ channelling by adding an alternative oxidase to submitochondrial particles and observing that it freely accepts electrons from NADH *via* CI and CoQ: on the basis of this finding, the authors suggest that the pathway involves the free CoQ pool even if CI is bound in an SC assembly.

Since the results of Hirst's group were obtained by oxygraphic measurements of oxygen consumption, they are potentially ambiguous since they depend on two subsequent pools, that of CoQ and that of cyt *c* Moreover, since in bovine mitochondria CIV appears to be functionally separate from CIII to large extent, we believe that the incomplete additivity of NADH and succinate fluxes is due to mixing at the level of the cyt *c* pool.

In a search for additional systems of investigation, we found that pig heart mitochondria reveal profound differences in the cyt *c* region that make them suitable for studies of additivity of NADH and succinate fluxes. Indeed, these mitochondria, contrary to bovine mitochondria, have a high flux control at the level of CIV and reveal complete additivity of NADH and succinate fluxes investigated by oxygraphic measurements. The results of this investigation support previous studies that restricted electron transfer in the CoQ region by using cyt *c* as acceptor, and exhibited total additivity of NADH and succinate fluxes (*cf.* Table II in ref. [6]).

The data provided from the kinetic approach in this study clearly demonstrate that two separate subsets of bound and free CoQ and/or CIII indeed govern the aerobic oxidation respectively of NADH and succinate. The data also suggest that the CoQ bound in the SC may become exchangeable with the free CoQ pool in the membrane under some particular conditions, such as making the CoQ pool over-reduced by lowering the electron output through CIII by Antimycin A (AA) inhibition. The elucidation of this kinetic behaviour of SCs can pave the way for new insights into countering mitochondrial dysfunctions [16].

2. Methods

2.1. Chemicals

Rotenone, antimycin A were purchased from Vinci-Biochem (Vinci, Italy). NADH, succinate, ascorbate (ASC), and *N*,*N*,*N*′,*N*′-tetramethyl-*p*-phenylenediamine dihydrochloride (TMPD), n-dodecyl-β-D-maltoside (DDM), cytochrome *c* were obtained from Sigma–Aldrich (Milan, Italy). Quartz double distilled water was used for all reagent solutions.

2.2. Preparation of the swine heart mitochondria

Swine hearts (*Sus scrofa domesticus*) were collected at a local abattoir and transported to the lab within 2 h in ice buckets at 0–4 °C. After removal of fat and blood clots as much as possible, approximately 30–40 g of heart tissue was rinsed in ice-cold washing Tris-HCl buffer (medium A) consisting of 0.25 M sucrose, 10 mM Tris(hydroxymethyl)-aminomethane (Tris), pH 7.4 and finely chopped into fine pieces with scissors. Each preparation was made from one heart. Once rinsed, tissues were gently dried on blotting paper and weighted. Then tissues were homogenized in medium B consisting of 0.25 M sucrose, 10 mM Tris, 1 mM EDTA (free acid), 0.5 mg/mL BSA fatty acid free, pH 7.4 with HCl at a ratio of 10 mL medium B per 1 g of fresh tissue. After a preliminary gentle break up by Ultraturrax T25, the tissue was carefully homogenized by a motor-driven teflon pestle homogenizer (Braun Melsungen Type 853,202) at 650 rpm with 3 up-and-down strokes. The mitochondrial fraction was then obtained by stepwise centrifugation (Sorvall RC2-B, rotor SS34). Briefly, the homogenate was centrifuged at 1000 ×*g* for 5 min, thus yielding a supernatant and a pellet. The pellet was re-homogenized under the same conditions as the first homogenization and re-centrifuged at 1000 ×*g* for 5 min. The gathered supernatants from these two centrifugations, filtered through four cotton gauze layers, were centrifuged at 10,500 ×*g* for 10 min to yield the raw mitochondrial pellet. The raw pellet was resuspended in medium A and further centrifuged at 10,500 ×*g* for 10 min to obtain the final mitochondrial pellet. The latter was resuspended by gentle stirring using a Teflon Potter Elvejehm homogenizer in a small volume of medium A, thus obtaining a protein concentration of 30 mg/mL [17]. All steps were carried out at 0–4 °C. The protein concentration was determined according to the colorimetric method of Bradford [18] by Bio-Rad Protein Assay kit II with BSA as standard. The mitochondrial preparations were then stored in liquid nitrogen.

2.3. Preparation of the beef heart mitochondria

Beef heart are obtained from a slaughterhouse within 1–2 h after the animal is slaughtered, and placed on ice. All subsequent procedures are carried out at 4 °C. Fat and connective tissues are removed and the heart tissue is cut into small cubes. Two hundred grams of tissues are passed through a meat grinder and placed in 400 mL of sucrose buffer (0.25-M sucrose, 0.01-M Tris–HCl, pH 7.8). The suspension is homogenized in a Waring blender for 5 s at low speed, followed by 25 s at high speed. At this stage, the pH of the suspension must be adjusted to 7.5 with 1 M Tris. The homogenate is centrifuged for 20 min at 1200 ×*g* to remove unruptured muscle tissue and nuclei. The supernatant is filtered through two layers of cheesecloth to remove lipid granules, and then centrifuged for 15 min at 26,000 ×*g*. The mitochondrial pellet obtained is resuspended in 4 volumes of sucrose buffer, homogenized in a tight-fitting Teflonglass Potter-Elvejhem homogenizer (clearance of 0.02 mm), and then centrifuged at 12,000 ×*g* for 30 min. The pellet is resuspended in the sucrose buffer and stored in liquid nitrogen, at a protein concentration of 40 mg/mL determined according to the colorimetric method of Bradford [18] by Bio-Rad Protein Assay kit II with BSA as standard.

2.4. Preparation of cytochrome c-deficient mitochondria

Suspensions of mitochondria at a protein concentration of 40 mg/mL, were frozen for a period of 1 to several days at −20 °C, in a storage medium (0.25 M sucrose, 10 mM Tris, pH 7.4 with HCl). Once thawed, the suspension was centrifuged at 26,000 ×*g* for 10 min. The pellet was suspended at a concentration of 20 mg/mL in a solution of 0.015 M KCl. The mitochondria were allowed to swell the hypotonic medium for 10 min, and then centrifuged 105,000 ×*g* for 15 min. The colourless supernatant liquid and the small dark layer of non-swollen mitochondria were discarded. The swollen mitochondria pellets were resuspended at a concentration of 20 mg/mL in 0.15 M KCl. The mitochondria, left in isotonic KCl medium for 10 min, were then centrifuged at 105,000 ×*g* for 15 min. The red supernatant, containing most of the extractable cyt *c* was decanted and the isotonic extraction with KCl was repeated two more times. The mitochondria of the pellet, deficient in cyt *c*, were suspended at a protein concentration of 20 mg/mL in a storage medium. Cyt *c* content of the extracts was determined spectrophotometrically with a coefficient of 18.5 $mM^{-1}{\cdot}cm^{-1}$ for the difference in absorbance at 550 nm between the oxidized and dithionite-reduced forms [19]. The concentration of endogenous cyt *c* extracted by osmotic shock from swine heart mitochondria was 1.05 ± 0.10 nmol/mg mitochondrial protein out of a total of 3.39 ± 0.14 nmol/mg mitochondrial protein.

2.5. Mitochondrial respiration assays

Freezing and thawing mitochondrial fractions were used to evaluate mitochondrial respiration. To evaluate mitochondrial respiration mitochondria were uncoupled (freeze-thawed) so that the ATP synthase cannot synthesize ATP. The inhibition of ATP synthase by oligomycin ruled out any possible concomitant effect on respiratory activity, while the absence of any effect after the addition of the protonophore FCCP confirmed that mitochondria were uncoupled. Moreover, the exogenous NADH oxidation can drive electron transfer by the respiratory complex. The effect of the reducing substrate NADH provides evidence that oxygen consumption is produced by fragmented mitochondrial membranes since NADH cannot enter intact mitochondria. Immediately after thawing, the mitochondrial fractions were used to evaluate mitochondrial respiration. The experimental conditions adopted ruled out any potential concomitant effect of changes in the transmembrane electrochemical gradient of H^+. To detect mitochondrial respiratory activities, the oxygen consumption rates were polarographically evaluated by Clark-type electrode using a thermostated Oxytherm System (Hansatech Instruments) equipped with a 1 mL polarographic chamber. The reaction mixture (120 mM KCl, 10 mM Tris-HCl buffer pH 7.2), maintained under Peltier at a fixed temperature (37 °C) and continuous stirring, contained 0.25 mg mitochondrial protein [20].

To evaluate the NADH-O_2 oxidoreductase activity, the mitochondrial oxidation was run under saturating substrate conditions (75 μM NADH) after 2 min of stabilization of the oxygen signal. Preliminary tests assessed that under these conditions O_2 consumption was suppressed by 2.5 μM rotenone, a known inhibitor of CI [21]. The succinate-O_2 oxidoreductase activity by CII was evaluated by detecting the succinate oxidation in the presence of 2.5 μM rotenone. The reaction was started by the addition of 10 mM succinate after 2 min of stabilization of the oxygen signal. Also in this case preliminary tests assessed that, under the conditions applied, succinate oxidation was suppressed by 0.4 μM antimycin A, a selective inhibitor of CIII [22]. Consistently, the combined NADH+succinate-O_2 oxidoreductase activity was evaluated in absence of rotenone. TMPD/ASC-O_2 oxidoreductase activity by CIV was evaluated in presence of 0.5 mM TMPD +2 mM ASC by detecting the cyt *c* oxidation in the presence of 1 μg/mL antimycin A. Preliminary tests assessed that under these conditions O_2 consumption was suppressed by 1.0 mM KCN, a known inhibitor of CIV [21].

2.6. Kinetic analysis

The IC_{50} values, namely the inhibitor concentration that causes half-maximal inhibition of the mitochondrial respiration activity, were calculated by fitting the % of residual mitochondrial respiration activity data without inhibitor and in the presence of increasing inhibitor concentrations to the IC_{50} four-parameter Eq. (1). In the latter, the enzyme activity (*y*) is a function of the inhibitor concentration (*x*); *range* is the difference between the maximal enzyme activity recorded (without inhibitor) and the residual mitochondrial respiration activity not inhibited by inhibitor concentration, defined as *background*, and *m* is a slope factor [23].

$$y = \frac{Range}{1 + \left(\frac{x}{IC_{50}}\right)^{m}} + Background \tag{1}$$

The plot of S/v (*y*-axis) *versus i*, inhibitor concentration (*x*-axis), yields a straight line. This line has an intercept of S/v_0 on the S/v axis, and an intercept of $-i_{0.5}$ on the *i* axis. The modified Cornish-Bowden plot, has the great advantage of allowing an accurate determination of the concentration of an inhibitor ($i_{0.5}$) that decreases the rate of an enzyme-catalysed reaction by 50 % [24].

The respiration activated by exogenous cyt *c* is evaluated by a curved reciprocal plot in which the enzyme reaction rate (*v*), namely the NADH-O_2 oxidoreductase or succinate-O_2 oxidoreductase activities, is transformed in the reciprocal increased mitochondrial respiration in the absence of exogenous cyt *c* ($1/\Theta$) plotted as a function of the reciprocal concentration of cyt *c* used a substrate (1/S) [25].

$$\frac{1}{v} = \frac{1}{V} + \frac{K^S_{m'}}{s}\frac{1}{V} + \frac{K^S_s K^S_{m'}}{s^2}\frac{1}{V} \tag{2}$$

where $K^S_{m'}$ is the Michaelis constant for cyt *c* acting as a substrate and K^S_s is the apparent dissociation constant of the complex containing the enzyme with the substrate bond as an activator. In order to assess the kinetic interaction of cyt *c* in oxidated (cyt c_{ox}) or reduced (cyt c_{red}) state with the enzyme complexes, Hill plots were built in selected cyt *c* ranges, namely according to the linear transformation of Hill Eq. (3).

$$log\frac{v}{Vmax - v} = -nH_i log[\text{cyt } c] + logK' \tag{3}$$

where *V*max and *v* represent the enzymatic reaction rates, respectively in the presence and in the absence of increased concentration of cyt *c* oxidated or reduced state and *K*′ or $[S]_{0.5}$ is the substrate concentration that yields half-maximal velocity. By plotting log *v*/(*V*max-i) *versus* log [cyt *c*] a straight line is obtained whose slope is Hill coefficient ($-nH_i$). In case $|nH_i| \neq 1$ multiple binding sites of the cyt *c* can be involved even if the nH_i value cannot stoichiometrically correspond to the binding sites [26]. Correlation coefficients were never lower than 0.95 thus confirming the linearity of all plots.

2.7. Metabolic flux control analysis

Determinations of flux control coefficients and threshold plots were performed by titrating the whole respiratory chain activity (*i.e.*, NADH-O_2 oxidoreductase activity or succinate-O_2 oxidoreductase activity) and single steps with inhibitor KCN for CIV (*i.e.*, TMPD/ASC-O_2 oxidoreductase activity). The inhibition curves were obtained with a non-linear regression fitting procedure performed on all the raw titration values of every set of experimental data using single exponential decay with offset (Eq. (4)). The equation for a single exponential decay is:

$$y = A_0 \bullet e^{-kt} \tag{4}$$

where A_0 is the initial value on *y*-axis and *k* is the rate constant at a fixed time (*t*) that corresponds to the slope of the exponential curve.

The control coefficient (C_i), which can have any value from 0.0 (for

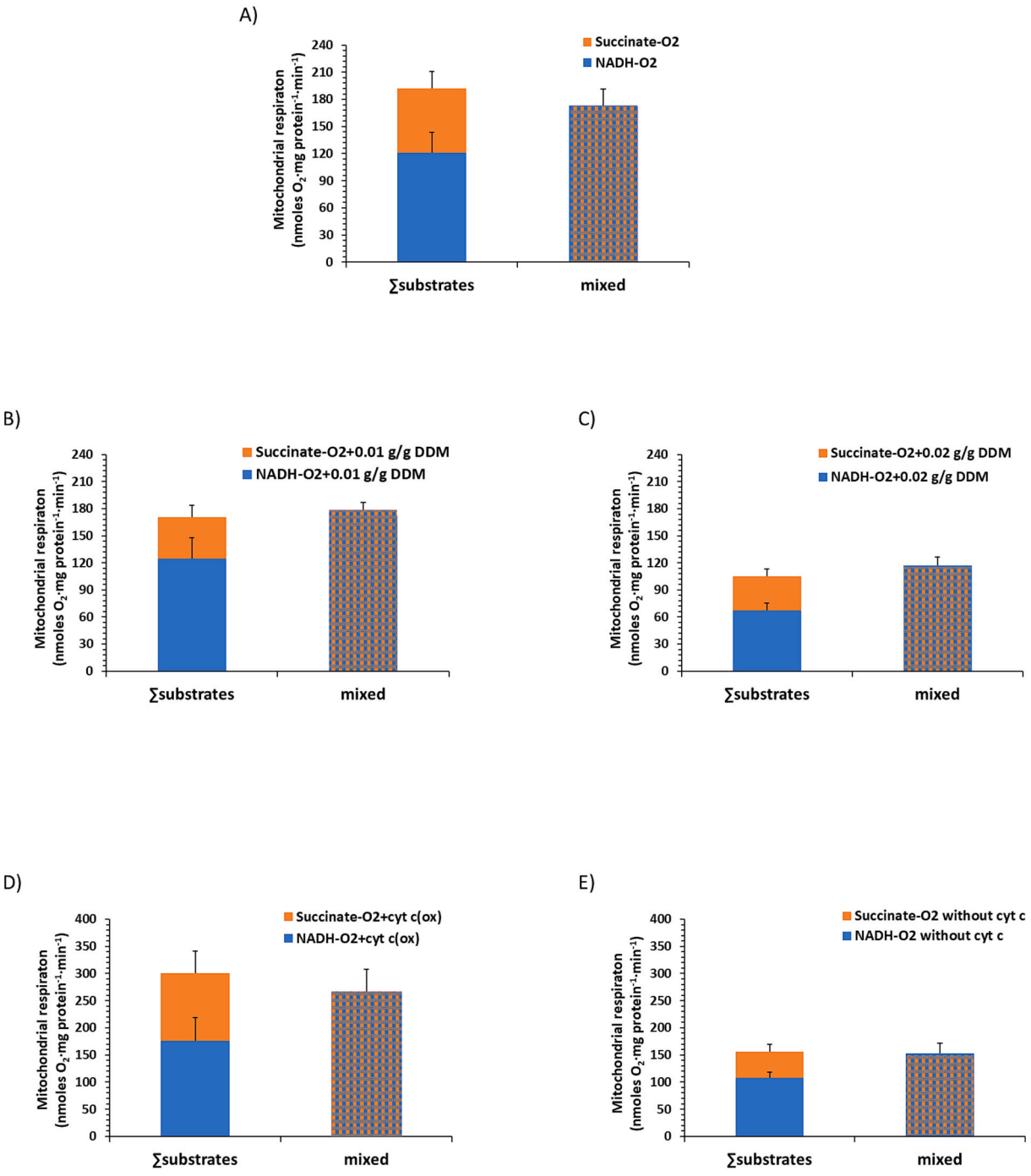

Fig. 1. Additivity of aerobic NADH and succinate oxidation. A) NADH-O_2 oxidoreductase and succinate-O_2 oxidoreductase activity summation (∑*substrates*) or NADH+succinate-O_2 oxidoreductase activities (*mixed*) in swine heart mitochondria (SHM). ∑*substrates* and *mixed* oxidoreductase activities in mitochondria solubilized with (B) 0.01 or (C) 0.02 g DDM on g of SHM, in presence of exogenous cyt c_{ox}, and with mitochondrial preparation without cyt *c*. Data represent the mean ± SD (vertical bars) from three independent experiments carried out on different mitochondrial preparations.

an enzyme with no impact on the flux) to 1.0 (for an enzyme that wholly determines the flux), was calculated from % changes of enzyme activities with the ratio of the initial slope of the inhibition curve of the global flux (J) to the initial slope of the inhibition curve of the individual step (v_i) upon the addition of different concentrations of specific inhibitors (I, *i.e.* KCN) accordingly Eq. (5).

$$C_i = \frac{\frac{dJ}{dI} I \to 0}{\frac{dv_i}{dI} I \to 0} \quad (5)$$

where $(dJ/dI)_{I\to0}$ is the initial slope of J and $(dv_i/dI)_{I\to0}$ is the initial slope of v_i. Threshold plots were derived from the titration curves by drawing the % rate of the global activity as a function of the inhibition percentage of the single step activity for the same inhibitor concentration [4].

2.8. Arrhenius plots

Arrhenius plots of the TMPD/ASC-O_2 oxidoreductase activity by CIV on swine or bovine heart mitochondria were built to evaluate the temperature dependence of the enzyme properties under study. To build such plots, the enzyme-specific activities, evaluated at 4–5 °C intervals

in the temperature range 8–37 °C, were taken as the expression of the reaction constant rate *k*. Accordingly, ln *k* was plotted against the reciprocal of the absolute temperature T (in °K), according to the linear form of Arrhenius Eq. (6):

$$ln\ k = lnA - \frac{E_a}{R}\frac{1}{T} \quad (6)$$

where *k* is the rate constant, *A* is the pre-exponential factor, E_a is the activation energy, *R* is the gas constant and T is the absolute temperature. As expected [27], as typical feature of membrane-bound enzymes, two intersecting straight lines were obtained. The activation energies above and below the point of discontinuity (break or melting temperature, Tm) were directly calculated from the slopes of the straight lines obtained, multiplied by the gas constant *R*. According to the units employed, the activation energies were then expressed as kcal/mol [26]. The correlation coefficients, never lower than 0.98, confirmed the linearity of all plots.

2.9. Calculations and statistics

The data represent the mean ± SD (shown as vertical bars in the figures) of the number of experiments reported in the figure captions. In each experimental set, the analyses were carried out on different pools of animals. Statistical analyses were performed by SIGMASTAT software. The analysis of variance followed by Students–Newman–Keuls' test when *F* values indicated significance ($P \leq 0.05$) was applied. Percentage data were arcsin-transformed before statistical analyses to ensure normality.

3. Results and discussion

3.1. Studies of the additivity of NADH and succinate fluxes in swine heart mitochondria

Freeze-thawed (uncoupled) mitochondria were energized in the presence of either NADH, succinate or NADH+succinate as substrates, which stimulate the activity of CI (NADH), CII (succinate) or CI and CII (NADH+succinate), respectively. By oxygraphic measurements of oxygen consumption on swine heart mitochondria, the existence of two separate pools of CoQ dedicated to NADH oxidation or succinate oxidation has been investigated. The sum of the two single steps, *i.e.* NADH-O_2 oxidoreductase and succinate-O_2 oxidoreductase activities, were the same as combined NADH+succinate-O_2 oxidoreductase activity (Fig. 1A) to support the existence of separate CoQ pools from NADH or succinate to CIII [4]. Indeed, the additivity of NADH and succinate activities should reduce the whole population of CoQ since the combined activity was not less than the sum of the individual rates. The existence of two distinct pathways indicated that there had to be some sort of compartmentalization of these flows, otherwise, they would have competed and exhibited pooling behaviour and, consequently, shown incomplete additivity.

This result was unexpected in consideration of the findings of Blaza et al. [12] in beef heart submitochondrial particles and mitochondrial membranes, showing incomplete additivity, and prompted us to further investigate our experimental system.

Mild detergents, such as DDM, are known to dissolve mainly the mitochondrial SCs in mammals containing CI, since the interaction of CIII and CIV is largely preserved [9]. Nevertheless, the mitochondria retained the NADH+succinate additivity in two solubilization conditions: in the first condition with 0.01 g/g DDM on mitochondrial protein in order to not affect the respiration (Fig. 1B) and in the second condition with 0.02 g/g DDM that was responsible for halving mitochondrial respiratory activities (Fig. 1C). Clearly, SCs in these mitochondria appear to be particularly resistant to detergents.

It was also considered the role of the cyt *c*, the second mobile electron

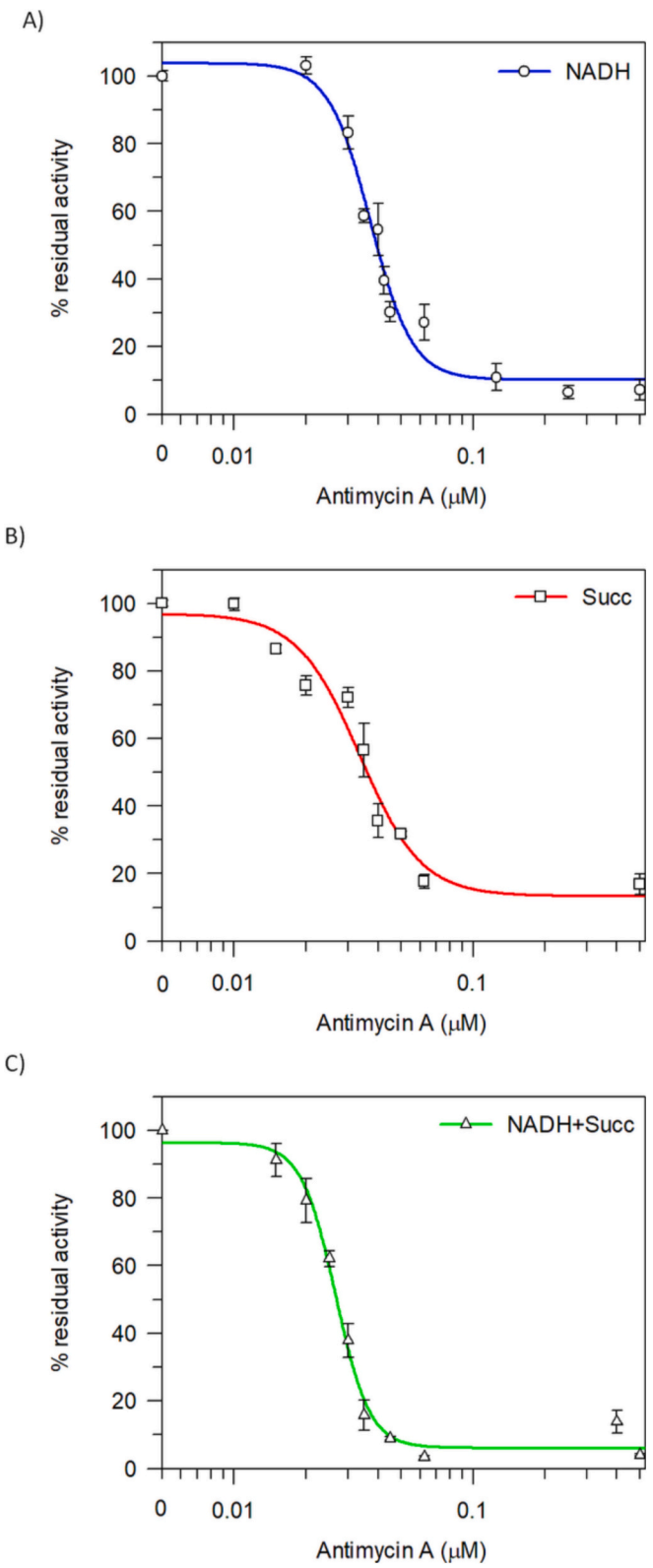

Fig. 2. Response of the mitochondrial respiration to antimycin A. The enzyme activity was assayed in the presence of 75 μM NADH, 10 mM succinate or both as substrates at different antimycin A concentrations. % residual activity of (A) NADH-O_2 oxidoreductase, (B) succinate-O_2 oxidoreductase, and (C) NADH+succinate-O_2 oxidoreductase activities are plotted against antimycin A concentrations (logarithmic scale). Data represent the mean ± SD (vertical bars) from three independent experiments carried out on different mitochondrial preparations.

Table 1
Antimycin A titrations analysis of the aerobic NADH and/or succinate in swine heart mitochondria.

Antimycin A (nM)	Substrate-O_2 oxidoreductase activity (nmoles O_2·mg protein^{-1}·min^{-1})		
	NADH	Succinate	NADH+succinate
0.0	133.7 ± 2.0	56.5 ± 0.5	202.4 ± 4.0*
20.0	137.9 ± 3.3	42.8 ± 1.6	105.9 ± 8.7*
30.0	111.3 ± 6.5	40.7 ± 1.7	50.5 ± 6.7*
35.0	78.5 ± 2.7	31.9 ± 4.5	21.1 ± 6.1*
40.0	73.0 ± 10.4	20.1 ± 2.8	18.5 ± 4.4*
45.0	40.4 ± 4.0	17.9 ± 0.4	11.9 ± 0.7*
62.5	36.3 ± 7.0	10.0 ± 1.1	4.4 ± 0.5*
500.0	9.7 ± 4.0	9.5 ± 1.7	5.4 ± 0.4*

Data are the mean ± SD of n = 3 sets of experiments carried out on different mitochondrial preparations.

* Indicate significant differences by missing additivity in NADH+succinate-O_2 oxidoreductase activity in presence of AA at $P \leq 0.05$.

carrier of the respiratory chain, that can form a bottleneck for electron flow directed to CIV. We performed experiments with the addition of oxidized cyt *c* (cyt $c_{(ox)}$) to mitochondria and evaluated the respiration by adding either NADH or succinate to mitochondria or adding both substrates simultaneously (Fig. 1D). The cyt $c_{(ox)}$ had the ability to increase the respiration activities if compared to mitochondrial respiration without exogenous cyt $c_{(ox)}$ (Fig. 1A), indicating that in these mitochondria the residual cyt *c* was not saturating, probably due to its loss during the freezing-thawing cycle. Indeed, in membrane mitochondria, the quantity of endogenous cyt *c* was 1.05 ± 0.10 nmol/mg mitochondrial protein (see Section 2.4). However, we detected the additivity of NADH+succinate-O_2 oxidoreductase activity also in this experimental condition (Fig. 1D). We tried to evaluate the mitochondrial respiration in cyt *c*-deficient mitochondria (Fig. 1E). The mitochondrial respiration in presence of NADH or succinate decrease about 20 %. Nevertheless, the NADH+succinate-O_2 oxidoreductase activity preserved the additivity. It is clear that these mitochondria maintain additivity of NADH and succinate oxidation in a variety of conditions; this observation suggests that two separate electron fluxes are kept in both the CoQ and cyt *c* regions, otherwise any mixing in either pool would prevent complete additivity. These data also suggest the possibility of channelling between CIII and CIV facilitated by SC formation [8], at difference with our previous results in beef heart mitochondria [4]. Indeed, in the space surrounding the $CIII_2CIV$ the cyt *c* can be maintained by weak electrostatic interactions between the positively charged cyt *c* and the negatively charged SC surface remaining in equilibrium with the cyt *c* pool [28].

In order to evaluate the effect of AA on mitochondrial respiration in presence of NADH or succinate as electron donors, the O_2 consumptions were evaluated in the range of 0.01–0.4 μM AA (Fig. 2). The substrate-O_2 oxidoreductase activities were strongly reduced by a sigmoidal concentration-response profile. The sigmoidal shape of the AA inhibition was ascribed by Kroger and Klingenberg [13] to the existence of a common diffusible pool of CoQ. The substrate-depending inhibition potency of AA, estimated as IC_{50} values, was calculated as 37.2 ± 1.6 nM for the NADH-O_2 oxidoreductase activity (Fig. 2A), 33.4 ± 3.2 nM for the succinate-O_2 oxidoreductase activity (Fig. 2B), and 26.6 ± 0.9 nM for the NADH+succinate-O_2 oxidoreductase activity (Fig. 2C). The IC_{50} values of AA on substrate oxidation highlighted that single NADH or succinate flux converging on CIII are equally inhibited. Conversely, the additivity of NADH and succinate oxidation created increased fluxes on the electron transport chain, as reported in Fig. 1, and consequently, the stimulated mitochondrial respiration was most affected by AA (Fig. 2C). These results are compatible with the existence of two separate fluxes for NADH and succinate in the CoQ region, since each individual substrate elicits a flux across an aliquot of the AA-inhibited molecules of CIII, whereas the combination of both substrates elicits a flux across all AA-inhibited CIII molecules.

On the other hand, even at low concentrations AA induces loss of additivity; inspection of Table 1 indicates that AA induces CoQ pool function. Presumably, NADH-reduced CoQ molecules that interact with inhibited CIII are dissociated from the Complex and homogenized in the common CoQ pool, so that they can interact with free non-inhibited CIII molecules; however, if succinate is present, the remaining non-inhibited molecules of CIII are unavailable for these interactions. The existence of a dissociation equilibrium of SC-bound CoQ with the CoQ pool was proposed by Genova and Lenaz [29] to become operative when the flux of electrons becomes interrupted at the level of CIII. Under normal flux conditions, CoQ reduced by CI within the SC is reoxidized by supercomplexed CIII, because presumably the dissociation rate constant k_{off} is slower than the rate constant of CIII reduction [29]; when CIII is inhibited the dissociation prevails and CoQ is dispersed in the pool.

3.2. *Flux control analysis for the respiratory complexes in swine and bovine heart mitochondria*

The finding of complete additivity of NADH and succinate fluxes in our system is at complete difference from the results of Blaza et al. [12] in beef heart mitochondrial membranes. In principle, the difference might be due to either the different kinds of mitochondria used or to different experimental conditions. In order to discriminate among these possibilities, we have decided to investigate other kinetic parameters and compare them in swine and bovine mitochondria. Our first demonstration of channelling was obtained by flux control analysis in beef heart mitochondria [4]: the finding that CI and CIII were equally rate-limiting in aerobic NADH oxidation was taken as an indication that they behave as a single enzyme (a SC); on the other hand, in this system, CIV was not limiting, suggesting that electron flow in that area is not or scarcely occurring by channelling. On the other hand, the data shown above in swine mitochondria strongly suggest that electron transfer from CIII to CIV occurs by channelling of cyt *c*. We have therefore decided to compare the flux coefficients of CIV in the two types of mitochondria.

The *global activity* identified as NADH-O_2 oxidoreductase activity and the specific activity of TMPD/ASC-O_2 oxidoreductase activity, which identifies the *individual step*, have been analyzed in swine heart mitochondria by titration with KCN, the specific inhibitor or CIV. The titration curve profile, which highlighted a single exponential decay, was similar for both NADH-O_2 and TMPD/ASC-O_2 oxidoreductase activity. Accordingly, the rate constants obtained from curves gradients with NADH or TMPD/ASC are 36.84 ± 6.82 and 45.18 ± 9.01, respectively. The C_i obtained by the ratio of the initial slopes is 0.82. The threshold plot obtained from experimental data of KCN titration depicted a residual NADH-O_2 oxidoreductase activity as a function of % inhibition of CIV that was linear (Fig. 3B). At high concentration of exogenous cyt *c* the C_i obtained were similarly high (0.86) and the threshold plots linear, indicating that the results do not depend on cyt *c* being rate-limiting in this system (Fig. 3C,D).

In the framework of metabolic control analysis, a typical behaviour highlights that CIV exerts complete control on the NADH-driven respiratory rate. This finding is the opposite with respect to our old data in beef mitochondria [4]. In fact, in bovine heart submitochondrial particles, we found that CIV minimally controls the aerobic oxidation of NADH: the threshold plot showed an evident breakage and a low C_i value [4]. We, therefore, tried to verify in our experimental condition on bovine heart mitochondria the flux control exerted by CIV over aerobic NADH oxidation determined using KCN to progressively inhibit the NADH-O_2 and TMPD/ASC-O_2 oxidoreductase activity. Different hyperbolic profiles were depicted and the rate constants obtained by curve initial slopes were 29.29 ± 6.42 and 109.39 ± 18.28 in the presence of NADH or TMPD/ASC, respectively. As a result, a lower $C_i = 0.27$ was measured for CIV highlighting that little control is exerted by the terminal enzyme of the respiratory chain in bovine heart mitochondria

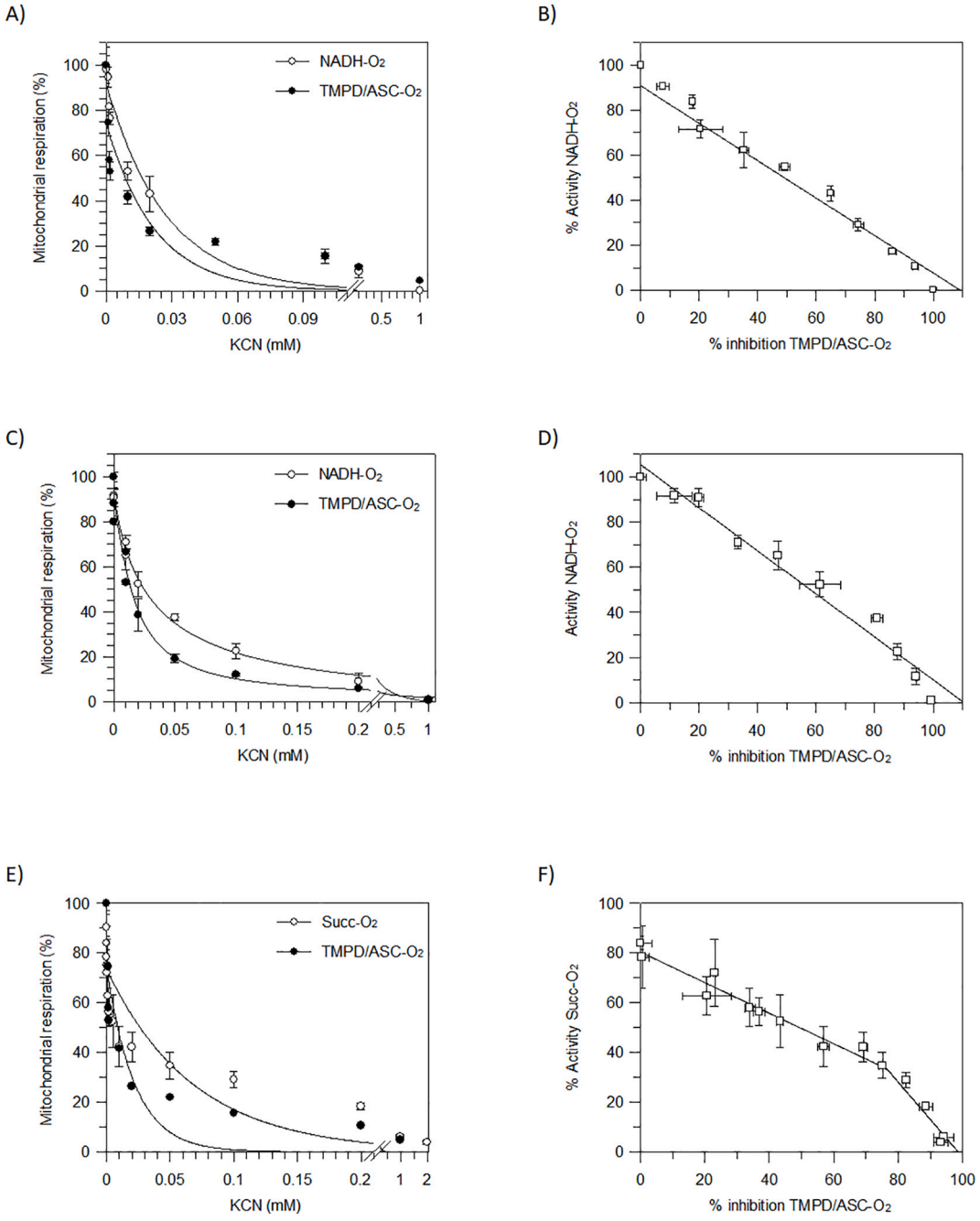

Fig. 3. Inhibitory KCN titrations analysis of the respiratory activities in swine heart mitochondria. Profile of *global* (–○–) with the stepwise inhibition of (A) NADH-O_2 oxidoreductase, (C) NADH-O_2 plus cyt *c* oxidoreductase or (E) succinate-O_2 oxidoreductase, and *specif* (–●–) with the stepwise inhibition of (A,E) TMPD/ASC-O_2 oxidoreductase or (C) TMPD/ASC-O_2 plus cyt *c* oxidoreductase activity. Threshold plots of (B) NADH, (D) NADH plus cyt *c*, and (F) succinate oxidase activity. Each point represents the % activity of aerobic NADH oxidation with CI (B) and aerobic succinate oxidation with CII (D) as a function of % inhibition of CIV for the same KCN concentration. The respiratory substrates sustaining the mitochondrial respiration were 75 μM NADH, 10 mM succinate, 0.5 mM TMPD +2 mM ASC, and 5 μM cyt *c*. All points represent the mean ± SD (vertical bars in A, C and E) and (vertical and horizontal bars in B, D and F) from three independent experiments carried out on different mitochondrial preparations.

(Fig. S1A). Consistently, the threshold plot presented a plateau phase followed by a steep breakage until CIV has been inhibited up to 70 % of its activity (Fig. S1B). Accordingly, by analyzing the combined and single aerobic NADH and succinate oxidation in this system, we found incomplete additivity (Fig. S1C), in total adherence with the data of Blaza et al. [12] in the same system, and corroborating the results of the metabolic flux control analysis. It is, therefore, demonstrated that swine and bovine heart mitochondria deeply differ in the kinetic properties of CIV, a further indication that the incomplete additivity of NADH and succinate fluxes found by Blaza et al. [12] results from mixing at the level of the cyt *c* pool. Indeed, the flux control analysis of Bianchi et al. [4] in beef mitochondria established that Complexes I and III have high flux control coefficients, whereas CIV has a low coefficient. This property of CIV has also been confirmed on NADH-O_2 oxidoreductase activity in our experiments. The logical interpretation is the presence of channelling in the I + III supercomplex of beef mitochondria, whereas electron transfer between CIII and CIV occurs largely by diffusion of cyt *c*. Moreover, the complete additivity of NADH and succinate oxidation by

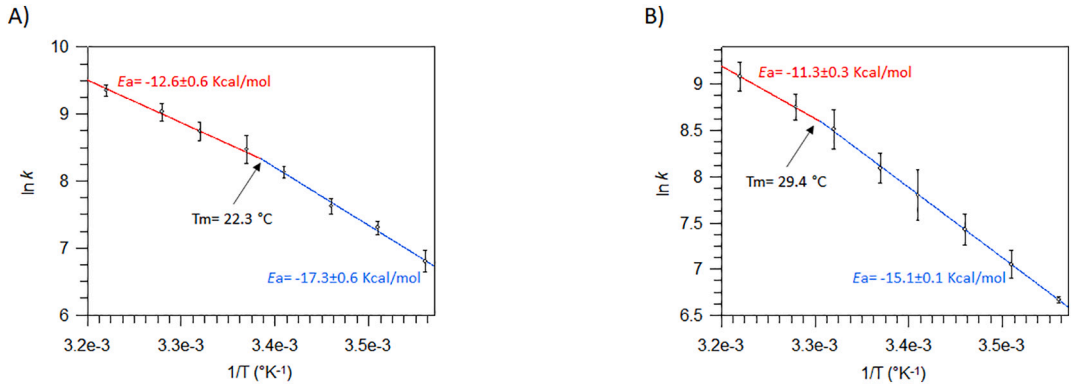

Fig. 4. Temperature dependence of the TMPD/ASC-O_2 oxidoreductase activity. Arrhenius plot in (A) swine and (B) bovine heart mitochondria. T_m indicates the temperature of the point of discontinuity (break) of the plot; Ea_1 and Ea_2 indicate the activation energies above and below T_m, respectively. Data are the mean ± SD (vertical bars) of three experiments carried out on different mitochondrial preparations.

exogenous cyt *c* in cyanide-inhibited bovine mitochondria found by Lenaz et al. [6] means that in these mitochondria there are two separate fluxes in the CoQ region, thus excluding the hypothesis that mixing occurs at the CoQ level.

Further analysis of the metabolic flux control of CII and CIV over the respiratory chain was performed by studying the variation of the succinate-O_2 and TMPD/ASC-O_2 oxidoreductase activity in mitochondria in the presence of KCN. The inhibition curves of the *global activity* (succinate-O_2 oxidoreductase) were not superimposable with the corresponding titration curves of CIV-specific activity (Fig. 3E). Therefore, in swine heart mitochondria, CIV exhibits a very low control over aerobic succinate oxidation, at difference with NADH oxidation where CIV exhibits high control. The rate constants with succinate and TMPD/ASC were 14.64 ± 4.68 and 45.28 ± 10.81, respectively. Indeed, the C_i was equal to 0.32 and the threshold plot was not linear (Fig. 3F). As previously shown in bovine mitochondria, the rate-limiting step is likely to be CII, however little control is exerted by CIV, suggesting that in the electron flux from succinate both the CoQ pool and the cyt *c* pool are largely employed, whereas in the oxidation of NADH the flux mostly takes place within the SC I-III_2-IV.

A study by Shimada et al. [30] compared the supercomplex composition from different sources including bovine heart and swine heart. The BN-PAGE studies showed a similar pattern with the presence of I + III_2 + IV supercomplexes, although the band for free CIV seems smaller in swine mitochondria. Nevertheless, it seems unlikely that the striking difference between bovine and swine CIV properties is merely due to a different proportion of SC-bound and free CIV. The different properties of the lipid membranes are likely able to modify the binding properties of cyt *c* to the membrane of the partner complexes.

We tried to explain the opposite results in the flux control exerted by CIV over aerobic NADH oxidation between swine and bovine heart mitochondria by considering biophysical differences in membrane features that could contribute to affecting the cyt *c* diffusion. We measured the temperature dependence of the TMPD/ASC-O_2 oxidoreductase activity showing that Arrhenius plots of swine and bovine heart mitochondria were discontinuous and showed a Tm at approximately 22.3 °C or 29.4 °C, respectively (Fig. 4A,B). The E_a above and below the break had a difference of about 2.5 Kcal/mol between swine and bovine heart mitochondria, being in both cases >25 % lower at temperatures above the Tm. The Arrhenius plot has long been known to be indicative of the

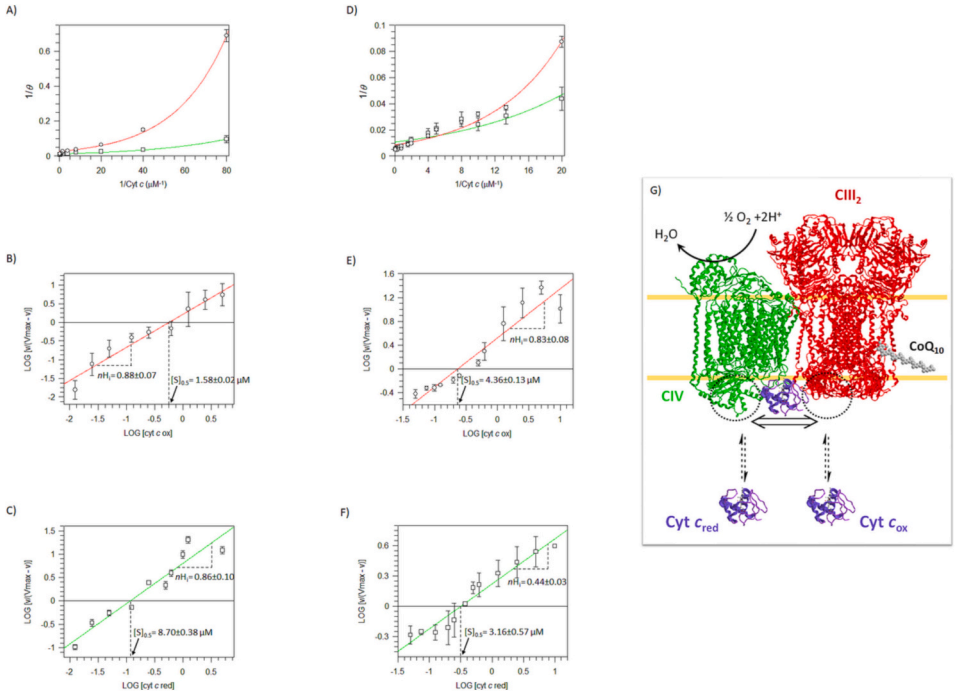

Fig. 5. Effect of exogen cyt *c* acting also as an activator of mitochondrial respiration. Activation of A) NADH-O_2 oxidoreductase and D) succinate-O_2 oxidoreductase activity in presence of cyt c_{ox} (—○—, red) and (C) cyt c_{red} —□—, green). Hill plots to obtain the kinetic parameters of the NADH-O_2 oxidoreductase activity in presence of exogenous (B) cyt c_{ox} and (C) cyt c_{red} or the succinate-O_2 oxidoreductase activity in presence of exogenous (E) cyt c_{ox} and (F) cyt c_{red}. Data represent the mean ± SD (vertical bars) from three independent experiments carried out on different mitochondrial preparations. G) Scheme illustrating how SC organization of CIII and CIV, drawn as ribbon representations obtained from modified Protein Data Bank ID: 2YBB, may be involved in the diffusion and exchange of cyt *c*.

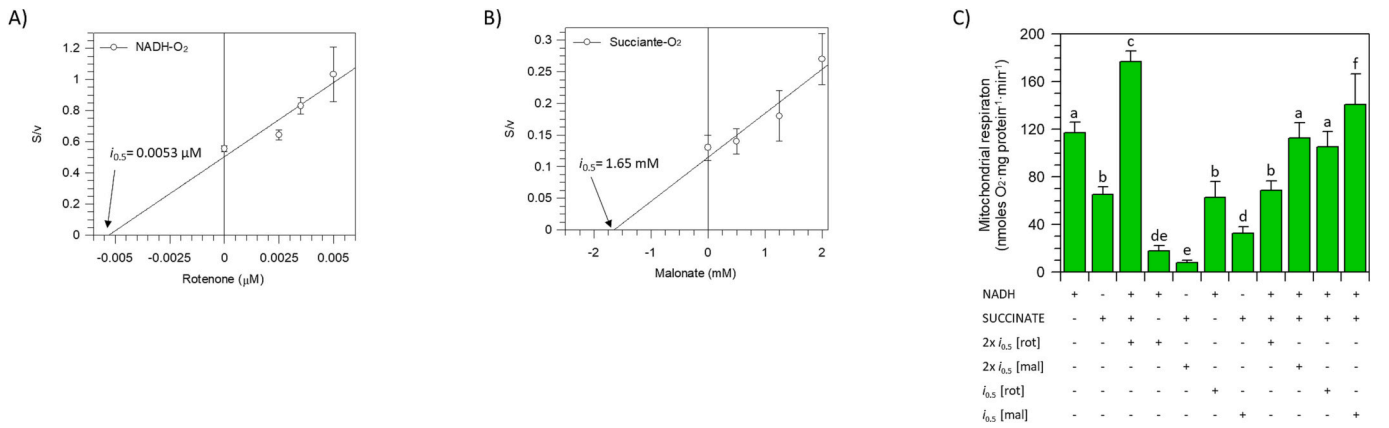

Fig. 6. Mitochondrial respiration activity in the presence of rotenone and malonate. A) NADH-O_2 oxidoreductase and B) succinate-O_2 oxidoreductase activity are plotted against increasing rotenone and malonate concentrations (logarithmic scale), respectively. Data plotted to determine the $i_{0.5}$ value. C) Effect of rotenone and malonate at fixed concentration on NADH or succinate and NADH plus succinate oxidation. Data are the mean ± SD (vertical bars) from three experiments carried out on different mitochondrial preparations. Different letters indicate significant differences ($P \leq 0.05$) among treatments with or without different concentrations of rotenone (rot) or malonate (mal).

membrane physical state [31]. Indeed, non-linear Arrhenius plots of mitochondrial membrane-bound enzymes showed transition temperatures that might be dependent on the degree of membrane-lipid unsaturation. The greater is the degree of lipid unsaturation, the lower is the transition temperature [32]. It is known that ruminants contain unsaturated fatty acids in the *trans* configuration or saturated fatty acids that both confer less fluidity to biological membranes. Therefore, the different degrees of unsaturation of the mitochondrial membrane of swine and bovine may play an important role in determining the properties of cyt *c* channelling. Further studies are required to investigate the lipid composition and its role in the determination of cyt *c* binding and SC formation.

3.3. Cyt c acting as an activator of $CIII_2CIV$

The interesting channelling of cyt *c* in SC of swine heart mitochondria has been studied in presence of exogenous cyt *c* in reduced (red) or oxidated (ox) form under NADH or succinate oxidation (Fig. 5). A concentration-dependent increase of NADH-O_2 oxidoreductase activity was registered (Fig. 5A). However, NADH oxidation with exogenous cyt c_{red} was about 26 % higher than mitochondrial respiration with exogenous cyt c_{ox}. NADH-O_2 oxidoreductase activity had an exponential profile independently of the redox state of exogenous cyt *c* suggesting the absence of inhibition by the substrate. By considering this trend we can assume that the total substrate concentration of cyt *c* was much lower than the total enzyme concentration. The data of NADH-O_2 oxidoreductase activity gave rise to a curved reciprocal plot rather than a straight line of Michaelis–Menten equation. This is the condition that characterizes a possible pathway in which the substrate is also the activator and the complex is composed of an enzyme-substrate-substrate activator (ESS_a). Combination with substrate and activator may be random- or compulsory-order, and equilibrium or steady-state conditions may exist [25]. It was therefore interesting to check the stoichiometry of the reaction catalysed to conclude if the complex kinetic exponential curves were due to cooperativity or not. The NADH-O_2 oxidoreductase activity stimulated by cyt c_{ox} or cyt c_{red} showed similar Hill coefficients, namely 0.88 ± 0.07 and 0.86 ± 0.10 respectively (Fig. 5B,C), thus suggesting that cyt c_{ox} or cyt c_{red} can bind to at one catalytic site to yield high rates of catalysis indifferently of redox state. Therefore, no cooperative binding was present. However, the site of cyt c_{ox} had a $[S]_{0.5}$ five times lower than cyt c_{red} (Fig. 5B,C). The difference could corroborate the level of activation of NADH-O_2 oxidoreductase activity with cyt c_{red} (Fig. 5A), in which more substrate was required to yield the maximal velocity.

The same activation effect has been detected in succinate-O_2 oxidoreductase activity although the difference in mitochondrial respiration activation in presence of exogenous cyt c_{ox} or cyt c_{red} (Fig. 5D) was not as evident as for the NADH oxidation. Moreover, a nH_i lower than 1.0 of succinate-O_2 oxidoreductase activity also confirmed one-site activation kinetics by supplementation of cyt c_{ox} or cyt c_{red}. Noteworthy, the values of $[S]_{0.5}$, specifically 4.36 ± 0.13 µM and 3.16 ± 0.57 µM which provided the cyt c_{ox} and cyt c_{red} concentration to achieve the half-maximal rate reaction of respiration, respectively, were not different as well as detected with the NADH-O_2 oxidoreductase activity. Since CII is not a component of SC III_2-IV and does not support the channelling of succinate-O_2 oxidoreductase activity (Fig. 3C,D), the NADH-O_2 oxidoreductase activity of respirosome and SC III_2-IV might have a different energy conversion involved in cyt *c* diffusion into the respiratory supercomplexes [8,33].

We might suppose that a tight cyt *c* is bound to $CIII_2CIV$ by shuttling between the two respiratory complexes as confirmed by the additivity results in prepared cyt *c*-deficient mitochondria (Fig. 1E) and the evidence of channelling in the metabolic flux control analysis (Fig. 3A,B). Moreover, exogenous cyt c_{ox} or cyt c_{red} can bind at only one binding site. Probably, cyt c_{ox} and cyt c_{red} are accepted by CIII and CIV, respectively (Fig. 5G).

3.4. Mobile electron carriers are not bottlenecks for electron flow

By using specific inhibitors of CI and CII, namely rotenone and malonate respectively, we extrapolated the inhibitor concentration that decreased the rate of an enzyme-catalysed reaction by 50 %, *i.e.* i_{50} [24]. The results obtained were 5.3 nM rotenone on NADH-O_2 oxidoreductase activity and 1.65 mM malonate on succinate-O_2 oxidoreductase activity (Fig. 6A,B). The behaviour of rotenone and malonate was explored by comparing the individual effect of one of the two inhibitors at twice or equal concentration of the respective $i_{0.5}$ on the additivity of NADH or succinate and NADH+succinate flux (Fig. 6C). In this diagnostic test, the combinate aerobic oxidation of NADH with succinate had full additivity of the NADH-O_2 plus succinate-O_2 oxidoreductase activity. By the addition of rotenone at the concentration that decreased the rate of NADH-O_2-catalysed reaction by 100 %, *i.e.* $2xi_{50}$ in order to block all the flux of NADH oxidation, the additivity of mitochondrial respiration had a residual activity comparable to the succinate-O_2 oxidoreductase activity. On the contrary, in presence of malonate at the concentration of $2xi_{50}$ the additivity decreased at the value of NADH-O_2 oxidoreductase activity. Consequently, the additivity of the combined rates of mitochondrial respiration in the presence of rotenone or malonate, at their

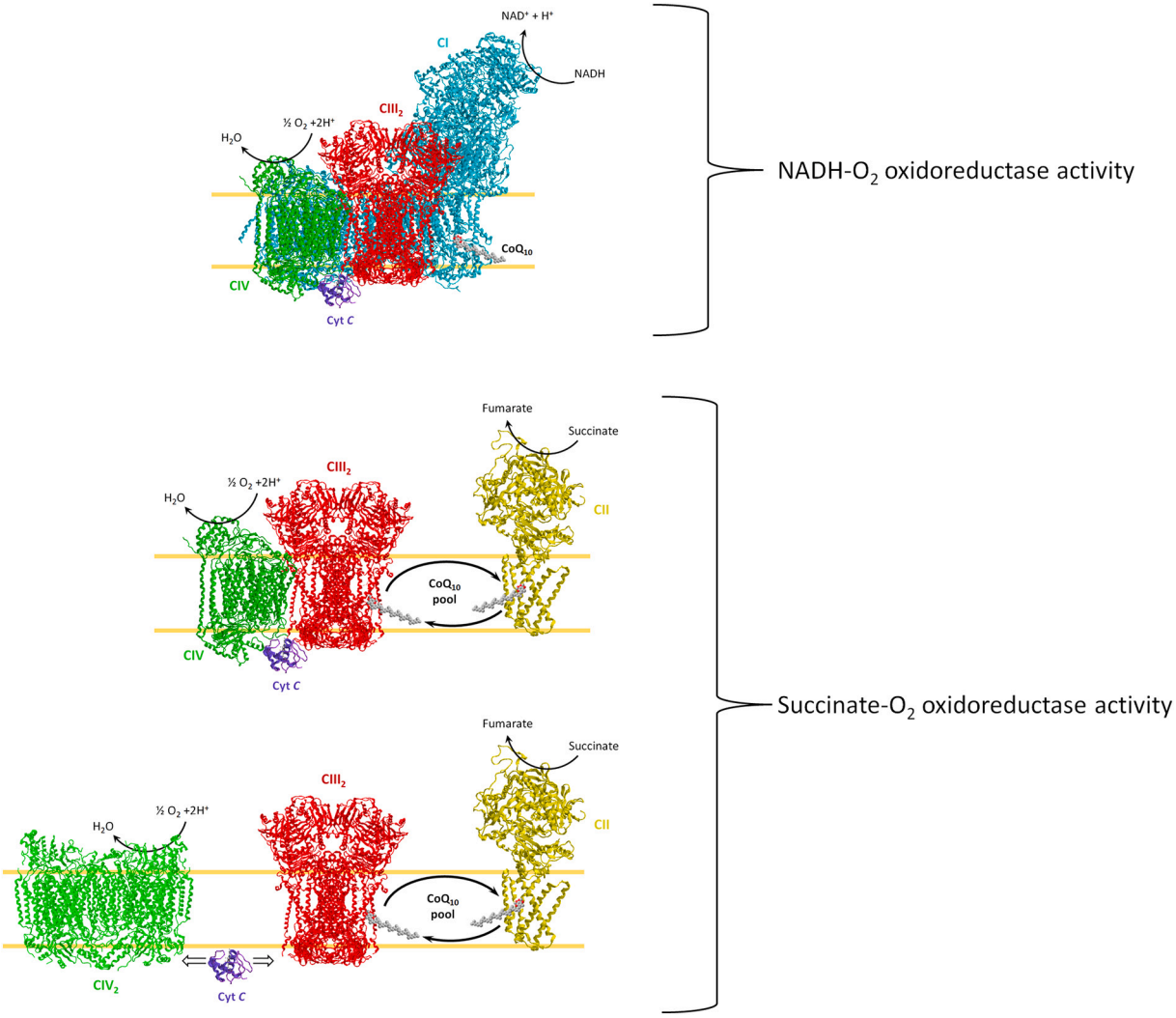

Fig. 7. Proposal of swine mitochondrial supercomplex to support the NADH-O_2 oxidoreductase ($I_1III_2IV_1$) or the succinate-O_2 oxidoreductase in the form of SC (II_1 + III_2IV_1) or as single respiratory complexes (II_1 + III_2 + IV_1). Fitted model by single particle cryo-EM. CoQ_{10} molecules are drawn in space-filling mode. Respiratory complexes are drawn as ribbon representations obtained from modified Protein Data Bank IDs: 2YBB and 1ZOY. The differently coloured letters identify the complex, drawn in the same colour as the letter.

respective i_{50} values, underwent a decrease in the reaction rate of substrates oxidation that corresponded to half of the respiratory activity with NADH or succinate, respectively (Fig. 6C). Thus, by decreasing the electron transport by inhibiting the initial complexes (CI or CII) the additivity is maintained, indicating that the two fluxes are independent under all conditions.

4. Conclusion

The experiments reported in this study demonstrate that, in swine heart mitochondria, NADH and succinate aerobic oxidation are characterized by two independent pathways, since the respective fluxes show complete additivity under a variety of conditions. These results are completely different from those obtained by Blaza et al. [12] in bovine heart mitochondrial membranes, in which the incomplete additivity was interpreted as adherence of the respiration rates to a homogeneous mobile pool of CoQ molecules.

Indeed, the flux of electrons from either NADH or succinate to oxygen must pass two potential pools of so-called mobile components, *i.e.*, CoQ and cyt *c*, and therefore the results are ambiguous in that they may reflect the pool properties of CoQ, cyt *c* or both. The older experiments in our laboratory using flux control analysis [4] in bovine heart mitochondrial membranes had shown a very small flux control exerted by CIV in contrast with the high values for CI and CIII, indicating the absence of channelling in the interaction between CIII and CIV: we suspect therefore that the incomplete additivity found by Blaza et al. [12] was due to mixing of the fluxes at the level of cyt *c*.

Moreover, when we repeated the flux control experiment in our preparation of swine heart mitochondria, we found a high flux control index for CIV, in adherence with the additivity data.

The difference of the present results in swine heart mitochondria with those of Blaza et al. on NADH and succinate additivity [12] and those of Bianchi et al. [4] on the flux control of CIV, both obtained in bovine heart mitochondria, may be due to either the different type of mitochondria or to some differences in the experimental conditions. For this reason, we repeated the experiments in bovine mitochondria under the same conditions, finding results in complete adherence with those obtained previously [4,12].

It is therefore clear that swine mitochondria exhibit an electron flow from NADH to O_2 that is completely independent and separated from the flow from succinate; indeed, this view is fully compatible with an electron flow within the I-III_2-IV respirasome.

If channelling occurs between CI and CIII by the common intermediate CoQ, the redox groups involved in CoQ reduction by CI and $CoQH_2$

re-oxidation in CIII must be in close contact in order to form a driving pathway containing CoQ itself; similar reasoning applies to cyt. *c* between CIII and CIV. An essential requirement for this condition is the availability of a high-resolution map of the molecular structure of the SCs. In several studies, purified SCs were analyzed by negative-stain electron microscopy and single-particle cryo-EM. According to Kuhlbrandt [34,35] the CoQ reduction site of CI in the SC is 11 nm far from the proximal CIII monomer. The linear CI arrangement with the active CIII monomer and with CIV is in favour of channelling in the respirasome by substrate micro-diffusion. On the other hand, the respirasome structure reported by Letts et al. [3,36] indicates that both CoQ interaction sites in CI and CIII are separated and easily accessible to the membrane, and are likely to provide no limit to free CoQ diffusion in the membrane. Therefore, channelling within the SC may occur by covering relatively long distances presumably by substrate-restricted diffusion (micro-diffusion) within the space between the two active sites; channelling necessarily occurs between two fixed sites of the same SC.

The structural analysis of SCs allows analogous considerations for cyt. *c* between CIII and CIV. In addition to our kinetic data in bovine mitochondria, also the structural evidence of purified SCs by cryo-EM adds structural reasons for the looseness of CIII–CIV interactions. In ovine mitochondria, Letts et al. [36] identified two distinct arrangements of SC I-III_2-IV: a major "tight" form and a minor "loose" form. In both structures, the density for CIV is weaker relative to that for CI and CIII, indicating the greater conformational flexibility of CIV. In the tight respirasome, CIV contacts both CI and CIII, whereas CIV in the loose respirasome has defined contacts only with CI.

In partial contrast with the above considerations, Lapuente-Brun et al. [10] demonstrated that at least part of CIV forms a functional SC with the channelling of cyt *c*, but the SC formation depends on the availability of the SC assembly factor SCAF1. Functional evidence for cyt *c* channelling was also found in *S. cerevisiae* [37] mitochondria which are characterized by having all CIV bound to CIII in a supercomplex [38], thus preventing electron transfer through free CIV units. The structural evidence by single particle cryo-EM sustains channelling, since in the III_2-IV_2 SC (there is no CI in this yeast species) the distance between the binding sites of cyt *c*, *i.e.*, cytochrome c_1 of CIII and the Cu_A-subunit II of CIV, is considerably shorter than that in bovine mitochondria [39]. Rydström Lundin et al. [40] demonstrated that the factor Rcf1 promotes the formation of a direct electron-transfer pathway from CIII to CIV *via* a tightly bound cyt *c*. Accordingly, in these mitochondria in the presence of added homologous cyt *c*, the direct cyt *c* channelling is faster than the equilibration of electrons with the cyt *c* pool. Consistently, direct channelling does not take place in a strain lacking Rcf1 and electrons are only transferred *via* the cyt *c* pool.

Analyzing the features of the electron flow from succinate to O_2, the results are somewhat different, since CIV exerts little control on succinate aerobic oxidation: this means that the respiration with succinate is supported by partial mixing not only at the CoQ level but also at the cyt *c* level (Fig. 7).

The different behaviour of swine and beef mitochondria is surprising in two closely related species (mammals); a possible reason may be in the different lipid composition, being the lipids from ruminants more saturated due to hydrogenation of their fatty acyl chains in the ruminants: the different membrane fluidity may change the binding of cyt *c* to the membrane or the tightness of the SCs.

Supplementary data to this article can be found online at https://doi.org/10.1016/j.bbabio.2023.148977.

CRediT authorship contribution statement

Salvatore Nesci: Conceptualization, Methodology, Validation, Formal analysis, Visualization, Project administration, Funding acquisition. **Cristina Algieri:** Methodology, Investigation, Writing – review & editing. **Fabiana Trombetti:** Methodology, Validation, Formal analysis, Writing – review & editing. **Micaela Fabbri:** Resources, Writing – review & editing. **Giorgio Lenaz:** Conceptualization, Methodology, Validation, Formal analysis, Writing – original draft, Supervision.

Declaration of competing interest

The authors declare that they have no known competing financial interests or personal relationships that could have appeared to influence the work reported in this paper.

Data availability

No data was used for the research described in the article.

Acknowledgements

Danilo Matteuzzi and Roberto Giusti (Department of Veterinary Medical Sciences, University of Bologna) are gratefully acknowledged for kindly conferring swine and bovine hearts from a local abattoir to Biochemistry laboratories.

This work was financed by the University of Bologna, RFO 2021 grant to SN.

References

[1] C.R. Hackenbrock, Ultrastructural bases for metabolically linked mechanical activity in mitochondria. I. Reversible ultrastructural changes with change in metabolic steady state in isolated liver mitochondria, J. Cell Biol. 30 (1966) 269–297, https://doi.org/10.1083/jcb.30.2.269.

[2] H. Schägger, K. Pfeiffer, Supercomplexes in the respiratory chains of yeast and mammalian mitochondria, EMBO J. 19 (2000) 1777–1783, https://doi.org/10.1093/emboj/19.8.1777.

[3] J.A. Letts, K. Fiedorczuk, L.A. Sazanov, The architecture of respiratory supercomplexes, Nature 537 (2016) 644–648, https://doi.org/10.1038/nature19774.

[4] C. Bianchi, M.L. Genova, G. Parenti Castelli, G. Lenaz, The mitochondrial respiratory chain is partially organized in a supercomplex assembly: kinetic evidence using flux control analysis, J. Biol. Chem. 279 (2004) 36562–36569, https://doi.org/10.1074/jbc.M405135200.

[5] M.L. Genova, A. Baracca, A. Biondi, G. Casalena, M. Faccioli, A.I. Falasca, G. Formiggini, G. Sgarbi, G. Solaini, G. Lenaz, Is supercomplex organization of the respiratory chain required for optimal electron transfer activity? Biochim. Biophys. Acta 1777 (2008) 740–746, https://doi.org/10.1016/j.bbabio.2008.04.007.

[6] G. Lenaz, G. Tioli, A.I. Falasca, M.L. Genova, Complex i function in mitochondrial supercomplexes, Biochim. Biophys. Acta Bioenerg. 2016 (1857) 991–1000, https://doi.org/10.1016/j.bbabio.2016.01.013.

[7] M.L. Genova, G. Lenaz, A critical appraisal of the role of respiratory supercomplexes in mitochondria, Biol. Chem. 394 (2013) 631–639, https://doi.org/10.1515/hsz-2012-0317.

[8] S. Nesci, G. Lenaz, The mitochondrial energy conversion involves cytochrome c diffusion into the respiratory supercomplexes, Biochim. Biophys. Acta Bioenerg. 1862 (2021), 148394, https://doi.org/10.1016/j.bbabio.2021.148394.

[9] R. Acín-Pérez, P. Fernández-Silva, M.L. Peleato, A. Pérez-Martos, J.A. Enriquez, Respiratory active mitochondrial supercomplexes, Mol. Cell 32 (2008) 529–539, https://doi.org/10.1016/j.molcel.2008.10.021.

[10] E. Lapuente-Brun, R. Moreno-Loshuertos, R. Aciń-Pérez, A. Latorre-Pellicer, C. Colaś, E. Balsa, E. Perales-Clemente, P.M. Quirós, E. Calvo, M.A. Rodríguez-Hernández, P. Navas, R. Cruz, Á. Carracedo, C. Lopez-Otín, A. Perez-Martos, P. Fernańdez-Silva, E. Fernańdez-Vizarra, J.A. Enríquez, Supercomplex assembly determines electron flux in the mitochondrial electron transport chain, Science 340 (2013) 1567–1570, https://doi.org/10.1126/science.1230381.

[11] R. Acin-Perez, J.A. Enriquez, The function of the respiratory supercomplexes: the plasticity model, Biochim. Biophys. Acta 2014 (1837) 444–450, https://doi.org/10.1016/j.bbabio.2013.12.009.

[12] J.N. Blaza, R. Serreli, A.J.Y. Jones, K. Mohammed, J. Hirst, Kinetic evidence against partitioning of the ubiquinone pool and the catalytic relevance of respiratory-chain supercomplexes, Proc. Natl. Acad. Sci. U. S. A. 111 (2014) 15735–15740, https://doi.org/10.1073/pnas.1413855111.

[13] A. Kröger, M. Klingenberg, Further evidence for the pool function of ubiquinone as derived from the inhibition of the electron transport by antimycin, Eur. J. Biochem. 39 (1973) 313–323, https://doi.org/10.1111/j.1432-1033.1973.tb03129.x.

[14] C.R. Hackenbrock, B. Chazotte, S.S. Gupte, The random collision model and a critical assessment of diffusion and collision in mitochondrial electron transport, J. Bioenerg. Biomembr. 18 (1986) 331–368, https://doi.org/10.1007/BF00743010.

[15] J.G. Fedor, J. Hirst, Mitochondrial supercomplexes do not enhance catalysis by quinone channeling, Cell Metab. 28 (2018) 525–531.e4, https://doi.org/10.1016/j.cmet.2018.05.024.

[16] S. Nesci, F. Trombetti, A. Pagliarani, V. Ventrella, C. Algieri, G. Tioli, G. Lenaz, Molecular and supramolecular structure of the mitochondrial oxidative

phosphorylation system: implications for pathology, Life 11 (2021) 242, https://doi.org/10.3390/life11030242.
[17] S. Nesci, V. Ventrella, F. Trombetti, M. Pirini, A. Pagliarani, The mitochondrial F1FO-ATPase desensitization to oligomycin by tributyltin is due to thiol oxidation, Biochimie 97 (2014) 128–137, https://doi.org/10.1016/j.biochi.2013.10.002.
[18] M.M. Bradford, A rapid and sensitive method for the quantitation of microgram quantities of protein utilizing the principle of protein-dye binding, Anal. Biochem. 72 (1976) 248–254.
[19] D.H. MacLennan, G. Lenaz, L. Szarkowska, Studies on the mechanims of oxidative phosphorylation. IX. Effect of cytochrome c on energy-linked processes, J. Biol. Chem. 241 (1966) 5251–5259.
[20] S. Nesci, C. Algieri, F. Trombetti, V. Ventrella, M. Fabbri, A. Pagliarani, Sulfide affects the mitochondrial respiration, the Ca2+-activated F1FO-ATPase activity and the permeability transition pore but does not change the Mg2+-activated F1FO-ATPase activity in swine heart mitochondria, Pharmacol. Res. 166 (2021), 105495, https://doi.org/10.1016/j.phrs.2021.105495.
[21] D.G. Nicholls, S.J. Ferguson, 5 - respiratory chains, in: D.G. Nicholls, S.J. Ferguson (Eds.), Bioenergetics, Fourth Edition, Academic Press, Boston, 2013, pp. 91–157, https://doi.org/10.1016/B978-0-12-388425-1.00005-1.
[22] S. Nesci, F. Trombetti, M. Pirini, V. Ventrella, A. Pagliarani, Mercury and protein thiols: stimulation of mitochondrial F1FO-ATPase and inhibition of respiration, Chem. Biol. Interact. 260 (2016) 42–49, https://doi.org/10.1016/j.cbi.2016.10.018.
[23] V. Ventrella, S. Nesci, F. Trombetti, P. Bandiera, M. Pirini, A.R. Borgatti, A. Pagliarani, Tributyltin inhibits the oligomycin-sensitive Mg-ATPase activity in Mytilus galloprovincialis digestive gland mitochondria, Comp. Biochem. Physiol. C Toxicol. Pharmacol. 153 (2011) 75–81, https://doi.org/10.1016/j.cbpc.2010.08.007.
[24] A. Cortés, M. Cascante, M.L. Cárdenas, A. Cornish-Bowden, Relationships between inhibition constants, inhibitor concentrations for 50% inhibition and types of inhibition: new ways of analysing data, Biochem. J. 357 (2001) 263–268, https://doi.org/10.1042/0264-6021:3570263.
[25] Malcolm Dixon, Edwin C. Webb, Enzymes, Third Edition, Academic Press, 1979.
[26] I.H. Segel, Enzyme kinetics, in: W.J. Lennarz, M.D. Lane (Eds.), Encyclopedia of Biological Chemistry, Academic Press, Waltham, 2013, pp. 216–220, https://doi.org/10.1016/B978-0-12-378630-2.00012-8.
[27] S. Nesci, V. Ventrella, F. Trombetti, M. Pirini, A. Pagliarani, Tributyltin-driven enhancement of the DCCD insensitive Mg-ATPase activity in mussel digestive gland mitochondria, Biochimie 94 (2012) 727–733, https://doi.org/10.1016/j.biochi.2011.11.002.
[28] A. Moe, J. Di Trani, J.L. Rubinstein, P. Brzezinski, Cryo-EM structure and kinetics reveal electron transfer by 2D diffusion of cytochrome c in the yeast III-IV respiratory supercomplex, Proc. Natl. Acad. Sci. U. S. A. 118 (2021), e2021157118, https://doi.org/10.1073/pnas.2021157118.
[29] G. Lenaz, M.L. Genova, Kinetics of integrated electron transfer in the mitochondrial respiratory chain: random collisions vs. solid state electron channeling, Am. J. Phys. Cell Phys. 292 (2007) C1221–C1239, https://doi.org/10.1152/ajpcell.00263.2006.
[30] S. Shimada, M. Oosaki, R. Takahashi, S. Uene, S. Yanagisawa, T. Tsukihara, K. Shinzawa-Itoh, A unique respiratory adaptation in Drosophila independent of supercomplex formation, BBA-Bioenergetics 1859 (2018) 154–163, https://doi.org/10.1016/j.bbabio.2017.11.007.
[31] J.K. Raison, J.M. Lyons, W.W. Thomson, The influence of membranes on the temperature-induced changes in the kinetics of some respiratory enzymes of mitochondria, Arch. Biochem. Biophys. 142 (1971) 83–90, https://doi.org/10.1016/0003-9861(71)90261-X.
[32] K. Watson, R.L. Houghton, E. Bertoli, D.E. Griffiths, Membrane-lipid unsaturation and mitochondrial function in Saacharomyces cerevisiae, Biochem. J. 146 (1975) 409–416, https://doi.org/10.1042/bj1460409.
[33] J. Berndtsson, A. Aufschnaiter, S. Rathore, L. Marin-Buera, H. Dawitz, J. Diessl, V. Kohler, A. Barrientos, S. Büttner, F. Fontanesi, M. Ott, Respiratory supercomplexes enhance electron transport by decreasing cytochrome c diffusion distance, EMBO Rep. (2020), e51015, https://doi.org/10.15252/embr.202051015.
[34] T. Althoff, D.J. Mills, J.-L. Popot, W. Kühlbrandt, Arrangement of electron transport chain components in bovine mitochondrial supercomplex I1III2IV1, EMBO J. 30 (2011) 4652–4664, https://doi.org/10.1038/emboj.2011.324.
[35] J.S. Sousa, D.J. Mills, J. Vonck, W. Kühlbrandt, Functional asymmetry and electron flow in the bovine respirasome, elife 5 (2016), https://doi.org/10.7554/eLife.21290.
[36] J.A. Letts, L.A. Sazanov, Clarifying the supercomplex: the higher-order organization of the mitochondrial electron transport chain, Nat. Struct. Mol. Biol. 24 (2017) 800–808, https://doi.org/10.1038/nsmb.3460.
[37] H. Boumans, L.A. Grivell, J.A. Berden, The respiratory chain in yeast behaves as a single functional unit, J. Biol. Chem. 273 (1998) 4872–4877, https://doi.org/10.1074/jbc.273.9.4872.
[38] J. Heinemeyer, H.-P. Braun, E.J. Boekema, R. Kouril, A structural model of the cytochrome C reductase/oxidase supercomplex from yeast mitochondria, J. Biol. Chem. 282 (2007) 12240–12248, https://doi.org/10.1074/jbc.M610545200.
[39] E. Mileykovskaya, P.A. Penczek, J. Fang, V.K.P.S. Mallampalli, G.C. Sparagna, W. Dowhan, Arrangement of the respiratory chain complexes in Saccharomyces cerevisiae supercomplex III2IV2 revealed by single particle cryo-electron microscopy, J. Biol. Chem. 287 (2012) 23095–23103, https://doi.org/10.1074/jbc.M112.367888.
[40] C. Rydström Lundin, C. von Ballmoos, M. Ott, P. Ädelroth, P. Brzezinski, Regulatory role of the respiratory supercomplex factors in Saccharomyces cerevisiae, Proc. Natl. Acad. Sci. U. S. A. 113 (2016) E4476–E4485, https://doi.org/10.1073/pnas.1601196113.